European Journal of Pharmacology 648 (2010) 50–58

Contents lists available at ScienceDirect

European Journal of Pharmacology

journal homepage: www.elsevier.com/locate/ejphar

Molecular and Cellular Pharmacology

Photodynamic activity of aloe-emodin induces resensitization of lung cancer cells to anoikis

Hong-Zin Lee [a,*], Wen-Hui Yang [b], Mann-Jen Hour [a], Chi-Yu Wu [c], Wen-Huang Peng [d], Bo-Ying Bao [a], Ping-Hsiu Han [a], Da-Tian Bau [e,*]

[a] School of Pharmacy, China Medical University, Taichung, Taiwan
[b] Department of Health Services Administration, China Medical University, Taichung, Taiwan
[c] Department of Internal Medicine, Chang-Hua Hospital, Chang-Hua, Taiwan
[d] Graduate Institute of Chinese Pharmaceutical Science, China Medical University, Taichung, Taiwan
[e] Terry Fox Cancer Research Laboratory, China Medical University Hospital, Taichung, Taiwan

ARTICLE INFO

Article history:
Received 28 May 2010
Received in revised form 10 July 2010
Accepted 24 August 2010
Available online 16 September 2010

Keywords:
Photosensitizer
Aloe-emodin
Anoikis
Lung cancer H460 cell
Intrinsic and extrinsic death pathway

ABSTRACT

Aloe-emodin was found to be a photosensitizer and possess anti-tumor activity. However, the detailed mechanism underlying the biological effects of aloe-emodin remains unknown. In this study, we explored the mechanisms of photocytotoxicity induced by aloe-emodin in lung cancer H460 cells. According to the results of the photoactivated aloe-emodin-induced disruption of cytoskeleton, we verify that aloe-emodin with irradiation induces anoikis of H460 cells. Photosensitized aloe-emodin-induced anoikis is associated with the protein expression of α-actinin and mitogen-activated protein (MAP) kinase members. In this study, a rapid opening of the mitochondrial permeability transition pore and the change in apoptosis-related protein expression were involved in photoactivated aloe-emodin-induced cell death. We also demonstrated that anoikis induced by aloe-emodin with irradiation is mediated through the intrinsic and extrinsic death pathways in a caspase-dependent manner in H460 cells.

1. Introduction

Photodynamic therapy is an effective therapy for local malignant tumors and involves a tumor-localizing photosensitizing agent, light and molecular oxygen (Castano et al., 2006; Morton et al., 2002). Recently, photodynamic therapy has been a treatment option for lung cancer that involves the administration of a photosensitizing agent and fiberoptic bronchoscope, which was used to deliver light to tumor tissue that has retained the agent (Jones et al., 2001; McCaughan, 1999). Aloe-emodin is an anthraquinone derivative similar to hypericin in structure, the third generation photosensitizer. Some reports have indicated that emodin anthrone is a precursor of the biosynthesis of hypericin (Bais et al., 2003; Zobayed et al., 2006). Cárdenas et al. (2006) also suggested that aloe-emodin could be a candidate drug for photodynamic therapy. Furthermore, our previous study demonstrated that 24 h of continuous exposure to 40 μM of aloe-emodin induced a typical apoptosis on lung cancer cells in the absence of light (Lee et al., 2001, 2005). Therefore, we anticipated that photosensitized aloe-emodin would exert a more potent anticancer effect than aloe-emodin alone did in human lung cancer cells.

Many reports indicated that cell anchorage not merely provides structural anchorage for a cell but also mediates pivotal survival signals (Frisch and Screaton, 2001; Schwartz, 1997). Therefore, the disturbance of cell anchorage will frequently lead to the immediate initiation of a suicide program, apoptosis, within the cell. However, apoptosis in response to lack of adhesion or inappropriate adhesion has been termed anoikis (Frisch and Francis, 1994). Furthermore, all the features that characterize apoptosis, including nuclear fragmentation and caspase activation are observed during anoikis (Frisch and Screaton, 2001). It has also been suggested that the acquisition of anoikis-resistance is regarded as a critical step during the metastatic growth of a tumor (Debnath et al., 2002; Swan et al., 2003). Therefore, resensitization of tumor cells to anoikis is of potential interest in designing anti-tumor therapies.

Apoptosis is a major form of cell death, which involves many factors such as expression of Bcl-2, caspases and mitogen-activated protein (MAP) kinase family proteins. The occurrence of apoptosis as a mechanism of photodynamic therapy-induced cell death has been previously demonstrated (Leung et al., 2008; Wu et al., 2006). Apoptosis has shown an association with the changes in cell morphology. The severe morphological changes in apoptotic cells suggest that apoptosis has dramatic implications on the cytoskeleton. Several reports have also demonstrated that the actin cytoskeleton plays an important role in the early stage of cell apoptosis (Leung et al., 2008; Soldani et al., 2007).

* Corresponding authors. Lee is to be contacted at School of Pharmacy, China Medical University, 91, Hsueh-Shih Road, Taichung, 40402, Taiwan. Tel./fax: +886 4 22316290.
E-mail address: hong@mail.cmu.edu.tw (H.-Z. Lee).

0014-2999/$ – see front matter © 2010 Elsevier B.V. All rights reserved.
doi:10.1016/j.ejphar.2010.08.033

The major purpose of this study was to examine the mechanisms of aloe-emodin-induced photocytotoxicity in H460 cells. We demonstrated that anoikis, a form of apoptosis, was induced by treatment with aloe-emodin and light through disruption of the cytoskeleton that is regulated by MAP kinase members and cytoskeleton-related proteins.

2. Materials and methods

2.1. Materials

Aloe-emodin, antipain, aprotinin, dithiothreitol, ethylene glycol bis (β-aminoethylether)-N,N,N′,N′-tetraacetic acid (EGTA), leupeptin, pepstatin, phenylmethylsulfonyl fluoride, Tris and TRITC (tetramethylrhodamine isothiocyanate)-conjugated phalloidin were purchased from Sigma Chemical Company (St. Louis, MO, USA). Annexin V-FITC apoptosis detection kit was purchased from BioVision (Mountain View, CA, USA). Antibodies to various proteins were obtained from the following sources: β-actin, Bcl-2 and HSP27 antibodies were purchased from Sigma Chemical Company; α-actinin, Bax, caspase-3, caspase-8, cytochrome *c*, ERK1, JNK and p38 were purchased from BD Biosciences (San Diego, CA, USA); caspase-7 was from Cell Signaling Technology (Beverly, MA, USA); caspase-9 was purchased from Abcam (Cambridge, MA, USA); and α-tubulin was purchased from Calbiochem (San Diego, CA, USA). HRP-conjugated goat anti-mouse and-rabbit IgG were from Jackson Immunoresearch (Hamburg, Germany).

2.2. Cell culture

H460 cells were grown in monolayer culture in Dulbecco's modified Eagle's medium (DMEM; Life Technologies, Rockville, MD, USA) containing 5% fetal bovine serum (FBS; HyClone, Logan, UT, USA), 100 U/ml penicillin and 100 μg/ml streptomycin (Gibco BRL, Rockville, MD, USA) and 2 mM glutamine (Merck, Darmstadt, Germany) at 37 °C in a humidified atmosphere comprised of 95% air and 5% CO_2. When H460 cells were treated with aloe-emodin, the culture medium containing 1% FBS was used.

2.3. Light source

The irradiation source was a set of fluorescent lamp (20 W, China Electric MFG. Corporation, Taiwan) located at a made-to-measure box. The wavelength of fluorescence lamp is in the range of 400–700 nm. The intensity of light was measured as Lux, a system international illumination measure. Lux was inverted to light dose (J/cm^2). The cells were irradiated at 40 W for 15, 30 and 60 min that correspond to 0.4, 0.8 and 1.6 J/cm^2 light dose, respectively.

2.4. Mitochondrial reductase activity

Cells were seeded at a density of 7×10^4 cells per well onto 12-well plate 48 h before being treated with drugs. H460 cells were incubated with 0.1% DMSO or with 10, 20 or 40 μM aloe-emodin for 4 h and then irradiated with 0.4, 0.8 or 1.6 J/cm^2 fluence dose. After irradiation, the cells were washed with phosphate-buffered saline (PBS). Cellular mitochondrial reductase activity of live H460 cells was determined by measuring the reduction of 3-(4,5-dimethylthiazol-2-yl)-2,5-diphenyltetrazolium bromide (MTT). At each end point, the treatment medium was replaced with fresh serum-free medium containing 2.4×10^{-4} M MTT at pH 7.4. Cells were incubated with MTT medium for 1 h at 37 °C. After solubilization in dimethylsulfoxide, absorbance was measured at 550 nm.

2.5. Morphological investigation

Cells were seeded at a density of 7×10^4 cells per well onto 12-well plate 48 h before being treated with drugs. H460 cells were incubated with 20 μM aloe-emodin for 4 h and then irradiated with various indicated fluence doses. After irradiation, the cells were immediately photographed with an Olympus IX 70 phase-contrast microscopy. A field was chosen in the center of each well at approximately the same location for photography.

2.6. Localization of F-actin

Cells grown on coverslips were treated with 0.1% DMSO or 20 μM aloe-emodin for 4 h and then irradiated with a fluence of 1.6 J/cm^2. After irradiation, medium was aspirated and cells were fixed in 3.7% formaldehyde in PBS for 15 min, followed by 3 min in acetone at −20 °C. Cells were permeabilized with 1% Triton X-100 in PBS for 10 min. The cells were gently washed with PBS. To visualize F-actin, the cells were incubated with 1.9×10^{-7} M TRITC-phalloidin in PBS for 40 min at room temperature. After three washings in PBS, the cells were observed by fluorescence microscopy (H600L, Nikon).

2.7. Immunostaining

Cells grown on coverslips were treated with 0.1% DMSO or 20 μM aloe-emodin for 4 h and then irradiated with 1.6 J/cm^2 fluence dose. After irradiation, cells were washed with PBS, fixed with formaldehyde for 10 min and then permeabilized with 1% Triton X-100 in PBS for 10 min. Fixed cells were subsequently incubated with a blocking solution (2.5% bovine serum albumin) for 1 h at room temperature. Cells were then incubated for 1 h at 37 °C with α-tubulin, α-actinin, HSP27 or p38 antibodies diluted 1:50 in TBST solution. The cells were washed 3 times with TBST and incubated for 30 min at 37 °C with fluorescein-conjugated anti-mouse or -rabbit IgG antibody diluted 1:50 in TBST. After washing with TBST, the specimens were mounted in glycerin and observed by fluorescence microscopy (H600L, Nikon).

2.8. Localization of microtubule

In this study, the detection of α- and β-tubulin was used to examine the microtubules in H460 cells. Cells grown on coverslips were treated with 0.1% DMSO or 20 μM aloe-emodin for 4 h and then irradiated with 1.6 J/cm^2 fluence dose. The detection of α-tubulin was performed by immunostaining assay. To detect β-tubulin, the cells were incubated for 30 min at 37 °C with 250 nM TubulinTracker™ Green reagent. After three washings in PBS, the cells were observed by fluorescence microscopy (H600L, Nikon).

2.9. Annexin V-FITC/PI double staining assay

Annexin V/PI staining assay was employed to further classify H460 cells in apoptosis or necrosis stages. Annexin V-FITC/PI double staining of the cells was determined using the annexin V-FITC apoptosis detection kit. Cells were seeded at a density of 4×10^5 cells onto 6-cm dish 48 h before being treated with drugs. H460 cells were incubated with 20 μM aloe-emodin for 4 h and then irradiated with various indicated fluence doses. For annexin-based FACS analysis, cells were trypsinized, washed twice in ice-cold PBS and resuspended in 500 μl binding buffer. Approximately 1×10^5 cells were then stained for 5 min at room temperature with annexin V-FITC and PI in a Ca^{2+} enriched binding buffer and analyzed by FACSCanto flow cytometer (Becton Dickinson, San Joes, CA, USA). Annexin V-FITC and PI emissions were detected in the FL 1 and FL 2 channels of FACSCanto flow cytometer, using emission filters of 520 and 623 nm, respectively. Approximately 10,000 counts were made for each sample. The percentages of distribution of normal (Q3), early

apoptosis (Q4), late apoptosis (Q2) and necrosis cells (Q1) were calculated by ModFit LT 3.0 Software (Verity Software House, Topsham, ME, USA).

2.10. Plasma membrane integrity

Plasma membrane integrity was measured by propidium iodide uptake. Cells were seeded at a density of 7×10^4 cells per well onto 12-well 48 h before being treated with drugs. H460 cells were incubated with 20 μM aloe-emodin for 4 h and then irradiated with 1.6 J/cm^2 fluence dose. After irradiation, cells were placed for 0, 30, 60 or 90 min in the dark and then the cells were immediately stained by 5 μM PI for 5 min at 37 °C. After three washings in PBS, the cells were observed by Olympus IX 70 fluorescence microscopy.

2.11. 4′,6-Diamidino-2-phenylindole dihydrochloride (DAPI) staining

H460 cells were seeded onto 12-well plate 48 h before being treated with drugs. The cells were incubated with 20 μM aloe-emodin for 4 h and then irradiated with 1.6 J/cm^2 fluence dose. After irradiation, cells were fixed with 3.7% formaldehyde for 15 min, permeabilized with 0.1% Triton X-100 and stained with 1 μg/ml DAPI for 5 min at 37 °C. The cells were then washed with PBS and examined by fluorescence microscopy (Olympus IX 70).

2.12. Measurement of mitochondrial permeability transition (MPT) pore with calcein

The opening of MPT pores in H460 cells was assessed by a modification of the method of Kajitani et al. (2007). Cells were seeded at a density of 4×10^5 cells onto 6-cm dish 48 h before being treated with drugs. H460 cells were loaded with 1 μM calcein-acetomethoxy ester for 30 min at 37 °C in 1 ml of DMEM supplemented with 1 mM $CoCl_2$. Cells were washed free of calcein and incubated with 0.1% DMSO or 20 μM aloe-emodin for 4 h and then irradiated with 1.6 J/cm^2 fluence dose. After irradiation, the fluorescence intensity of calcein was measured with FACSCanto flow cytometer (excitation, 488 nm; emission, 530 nm; Becton Dickinson, San Joes, CA, USA) and analyzed using ModFit LT 3.0 Software (Verity Software House, Topsham, ME, USA).

2.13. Protein preparation

Cells were seeded at a density of 1.3×10^6 cells onto 10-cm dish 48 h before being treated with drugs. H460 cells were incubated with 20 μM aloe-emodin for various indicated times and then irradiated with 1.6 J/cm^2 fluence dose. After irradiation, adherent and floating cells were collected at the indicated time intervals and washed twice in ice-cold PBS. Cell pellets were resuspended in cell lysis buffer (50 mM Tris–HCl, pH 7.5, 150 mM NaCl, 1% Nonidet P-40, 0.25% sodium deoxycholate, 1 mM EGTA, 1 mM dithiothreitol, 1 mM phenylmethylsulfonyl fluoride, 1 mM sodium orthovanadate, 1 mM sodium fluoride, 5 μg/ml aprotinin, 5 μg/ml leupeptin and 5 μg/ml antipain) for 30 min at 4 °C. Lysates were clarified by centrifugation at 1500 *g* for 30 min at 4 °C and the resulting supernatant was collected, aliquoted and stored at −80 °C until assay. The protein concentrations were estimated with the Bradford method.

2.14. Western blot analysis

Samples were separated by various indicated concentrations of sodium dodecyl sulfate-polyacrylamide gel electrophoresis (SDS-PAGE; Bio-Rad, Hercules, CA, USA). The SDS-separated proteins were equilibrated in transfer buffer (50 mM Tris–HCl, pH 9.0–9.4, 40 mM glycine, 0.375% SDS and 20% methanol) and electrotransferred to Immobilon-P Transfer Membranes (Millipore Corporation, Bedford, MA, USA). The blot was blocked with a solution containing 5% nonfat dry milk in Tris-buffered saline (10 mM Tris–HCl and 150 mM NaCl) with 0.05% Tween 20 (TBST) for 1 h, washed and incubated with antibodies to β-actin (1:5000, the detection of β-actin was used as an internal control in all of the data of Western blotting analysis), AIF (1:1000), Bax (1:500), Bcl-2 (1:1000), caspase-3 (1:1000), caspase-7 (1:2000), caspase-8 (1:8000), caspase-9 (1:200), cytochrome *c* (1:5000), ERK1 (1:5000), JNK (1:1000) and p38 (1:2500). Secondary antibody consisted of a 1:20,000 dilution of horseradish peroxidase (HRP)-conjugated goat anti-mouse IgG (for β-actin, Bcl-2, Bax, caspase-3, caspase-8, cytochrome *c*, ERK1, JNK and p38) or HRP-conjugated goat anti-rabbit IgG (for AIF, caspase-7 and caspase-9). The enhanced chemiluminescent (NEN Life Science Products, Boston, MA, USA) detection system was used for immunoblot protein detection.

2.15. Statistical analysis

All experiments were carried out at least three times. Each sample was tested in triplicate. The results are expressed as percentage ± S.D. of control. Statistically significant differences from the control group were identified by Student's *t* test for paired data. A *P* value less than 0.05 was considered significant for the all tests.

3. Results

3.1. Photoactivated cytotoxicity of aloe-emodin in lung cancer H460 cells

Since aloe-emodin is a photosensitizer, the present study served to evaluate the effect of aloe-emodin on photocytotoxicity of H460 cells in irradiation condition. We determined the effect of aloe-emodin on cell phototoxicity by mitochondrial reductase activity assay. The data are presented as proportional viability (%) by comparing the treated group with the untreated group, the viability of which was assumed to be 100%. Fig. 1A shows the results of MTT assay on H460 cells after a photodynamic treatment (various indicated concentrations of aloe-emodin for 4 h and then irradiated with various indicated fluence doses). The cell death is drug- and fluence dose-dependent. As shown in Fig. 1A, there is 40% cell death of H460 cells after pretreatment with 20 μM aloe-emodin for 4 h and then irradiation with 1.6 J/cm^2 light dose. Since H460 cells rapidly underwent cell death when triggered by aloe-emodin and light, LD40 (the concentration lethal to 40% of the cells), which was about 20 μM aloe-emodin and 1.6 J/cm^2 fluence dose, was chosen for further experiments. Cytotoxic effects in the absence of light (0 J/cm^2) were studied using different concentrations of aloe-emodin (10, 20 and 40 μM) for 4 h. Aloe-emodin did not show any dark toxicity at the evaluated concentrations determined by MTT assay (Fig. 1A). The phenotypic characteristics of aloe-emodin-sensitized/irradiated H460 cells were also evaluated by microscopic inspection of overall morphology. Cells treated with aloe-emodin and light showed a marked change in the cellular morphology. When cells were incubated with aloe-emodin (20 μM, 4 h) prior to irradiation (1.6 J/cm^2), a greater percentage of the cells displayed a rounded morphology (Fig. 1B). The swollen cells with many protuberances on cell's periphery were observed after 60 min irradiation (1.6 J/cm^2) of the aloe-emodin-sensitized cells. After treatment with 20 μM aloe-emodin in the dark, the cells appear well-spread and grow as groups of cells (Fig. 1B). In order to compare the activity of aloe-emodin with that of an approved photosensitizer, the photocytotoxic activity of 5-aminolevulinic acid (5-ALA) was evaluated in this study. 5-ALA, a second generation photosensitizer, is the precursor of endogenous protoporphyrin IX in the heme biosynthesis pathway. As shown in Fig. 1C, treatment with 3 mM 5-ALA for 4 h and 1.6 J/cm^2 light dose resulted in about 40% cell death of H460 cells.

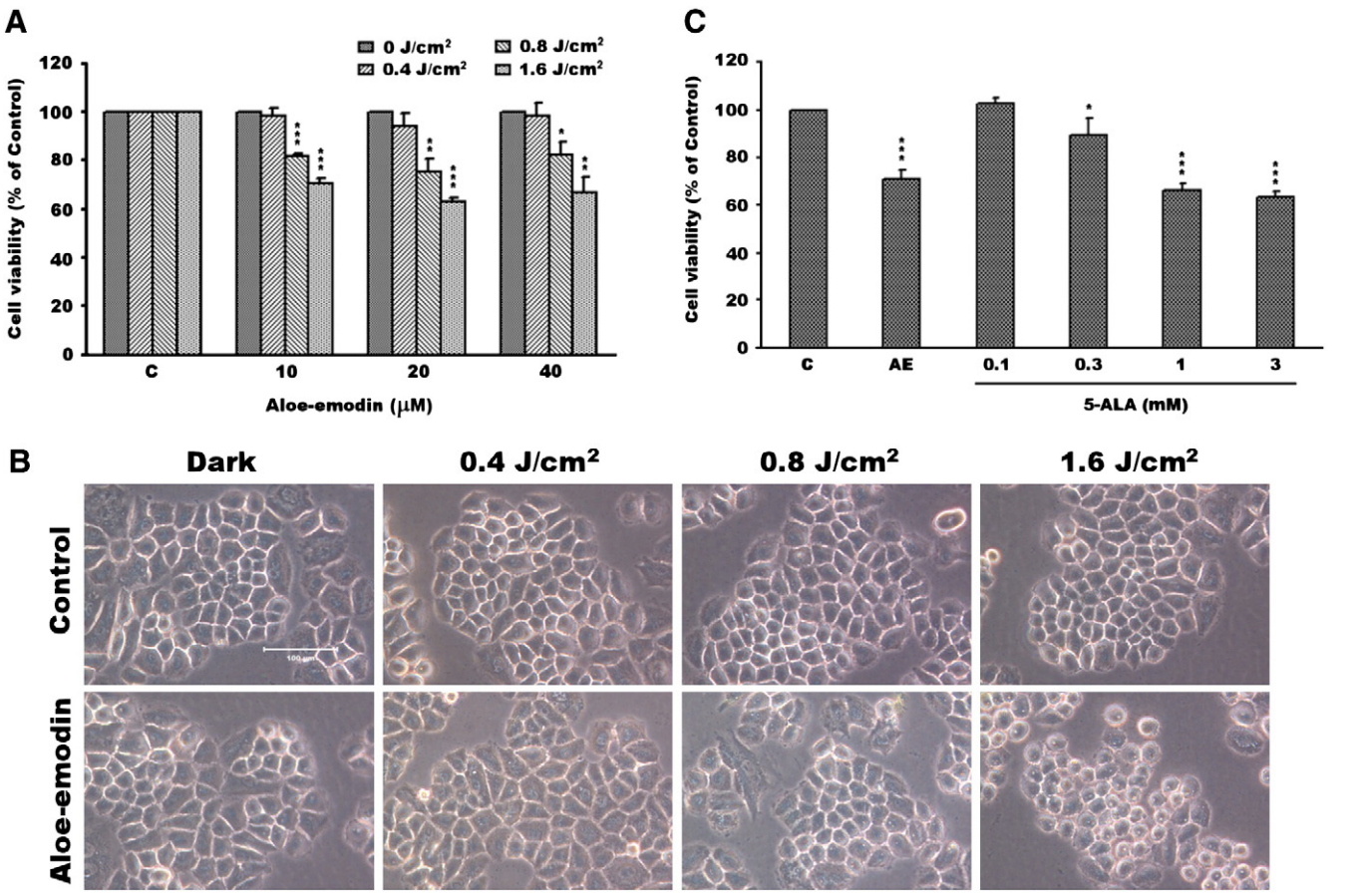

Fig. 1. Photoactivated cytotoxicity of aloe-emodin or 5-aminolevulinic acid in H460 cells. (A) Photodynamic effect of aloe-emodin on cell death of H460 cells. Cells were incubated with 0.1% DMSO or with 10, 20 or 40 μM aloe-emodin for 4 h and then irradiated with 0, 0.4, 0.8 or 1.6 J/cm^2 fluence dose. (B) Morphological analysis by phase-contrast microscopy of H460 cells. Cells were incubated with 0.1% DMSO or 20 μM aloe-emodin for 4 h and then irradiated with 0.4, 0.8 or 1.6 J/cm^2 fluence dose. After irradiation, the cells were immediately photographed with a phase-contrast microscopy. In light-shield condition, cells were incubated with 0.1% DMSO or 20 μM aloe-emodin for 4 h. (C) The effect of 5-aminolevulinic acid on photocytotoxicity of H460 cells. Cells were incubated with 0.1% DMSO, aloe-emodin (AE; 20 μM) or 5-aminolevulinic acid (5-ALA; 0.1, 0.3, 1 or 3 mM) for 4 h and then irradiated with 1.6 J/cm^2 fluence dose. All results are expressed as the mean percentage of control ± S.D. of triplicate determinations from four independent experiments. $^*P<0.05$, $^{**}P<0.01$, $^{***}P<0.001$ compared to the corresponding control values.

3.2. Photoactivation of aloe-emodin triggered disruption of microfilaments and microtubules in H460 cells

Based on the photosensitized aloe-emodin-induced morphological changes, we examined whether the cytoskeleton is the target of aloe-emodin with irradiation in H460 cells. The effect of photosensitized aloe-emodin on H460 cell actin microfilaments was examined using TRITC-phalloidin, a specific F-actin fluorescent probe. Actin microfilaments were present diffusely as short actin microfilaments throughout the control cells and pronounced accumulation of microfilaments at the cell periphery (Fig. 2A). After incubation with 20 μM aloe-emodin for 4 h and 1.6 J/cm^2 of fluence dose, fibers were thinner and often aligned parallel to each other and to the long axis of the cells (Fig. 2B). Microtubules and actin microfilaments are the major proteins of cytoskeleton and both regulate cell shape. To further examine whether the microtubules were injured by aloe-emodin with irradiation in H460 cells, TubulinTracker™ Green reagent was used to detect the β-tubulin of microtubule in this study. As shown in Fig. 2D, microtubules were present as short fragments throughout the cells after treatment of H460 cells with 20 μM aloe-emodin and 1.6 J/cm^2 light dose. However, β-tubulin is extensively fibrillar and localized mainly in perinuclear regions in the control cells (Fig. 2C). In this study, the aberration of α-tubulin expression involved in the photosensitized aloe-emodin-induced H460 cell death was also demonstrated. Studies with the anti-α-tubulin antibody showed that photoactivation of aloe-emodin caused severe disruption and breakage of H460 cell microtubules compared to those in control cells (Fig. 2F). In control cells, α-tubulin organized into punctate aggregates dispersed randomly throughout the cytoplasm and concentrated prominently on the one side of nuclear margin (Fig. 2E). These results demonstrated that aloe-emodin with irradiation induced the damage of cytoskeleton such as actin microfilaments and microtubules in H460 cells.

3.3. Photodynamic effects of aloe-emodin on the expression of α-actinin, p38 and HSP27 in H460 cells

Since cytoskeletal proteins are essential for regulation of cytoskeletal remodeling, the effects of photosensitized aloe-emodin on the expression of cytoskeletal regulatory proteins were directly assessed by immunostaining assay. In this study, we investigated the localization of α-actinin, which is an actin-cross-linking protein and may be critical for mediating the interaction between actin filaments and various cytoskeletal proteins, during photosensitized aloe-emodin-induced H460 cell death. Fig. 3A illustrates the α-actinin distribution of H460 cells in the control, where α-actinin organized into continuous aggregates dispersed randomly throughout the cells and aligned especially parallel to each other at the cell periphery. After treatment of H460 cells with 20 μM aloe-emodin and 1.6 J/cm^2 fluence dose, α-actinin is diffusely localized throughout the cells with no obvious organization (Fig. 3B). It has been reported that the cytoskeleton can be modulated by heat shock protein 27 (HSP27),

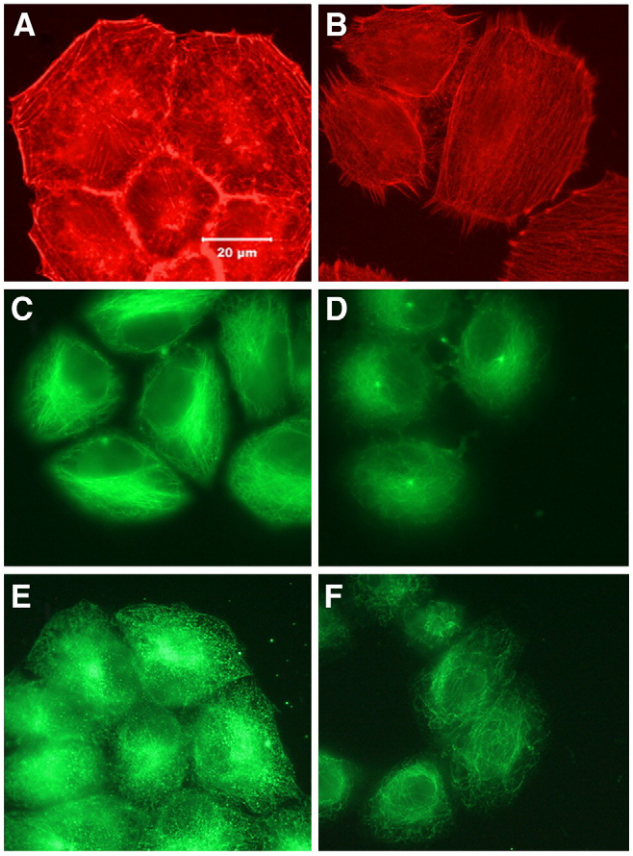

Fig. 2. Photodynamic effects of aloe-emodin on H460 cell cytoskeleton. Cells were incubated with 0.1% DMSO (A, C and E) or 20 μM aloe-emodin (B, D and F) for 4 h and then irradiated with 1.6 J/cm^2 fluence dose. After irradiation, the localization of F-actin (A and B), β-tubulin (C and D) and α-tubulin (E and F) was examined. To visualize F-actin, the cells were fixed, permeabilized and incubated with 1.9×10^{-7} M TRITC-phalloidin for 40 min. To examine β-tubulin, the cells were incubated for 30 min at 37 °C with 250 nM TubulinTracker™ Green reagent. To detect α-tubulin, the cells were incubated with mouse monoclonal anti-α-tubulin antibody as described in Section 2. The specimens were observed by fluorescence microscopy. Results are representative of three independent experiments.

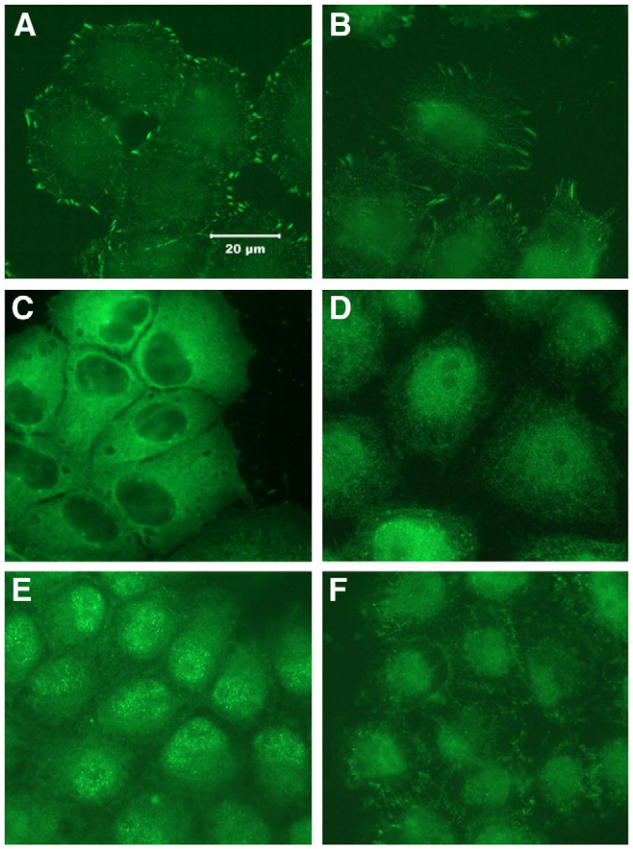

Fig. 3. Effects of photoactivation of aloe-emodin on the localization of α-actinin, HSP27 and p38 in H460 cells. The localization of α-actinin (A and B), HSP27 (C and D) and p38 (E and F) was performed by immunostaining in H460 cells. Cells were incubated with 0.1% DMSO (A, C and E) or 20 μM aloe-emodin (B, D and F) for 4 h and then irradiated with 1.6 J/cm^2 fluence dose. After irradiation, fixation and permeabilization, the immunostain of cells was performed with protein-specific antibodies as described in Section 2. The specimens were observed by fluorescence microscopy. Results are representative of three independent experiments.

which can interact with actin, and p38 interacts with the actin cytoskeleton via the HSP27. This study investigated the protein localization of HSP27 and p38 during aloe-emodin-induced H460 cell death. In the HSP27 staining studies, a marked nuclear localization of the HSP27 was observed in aloe-emodin-photosensitized cells (Fig. 3D). As shown in Fig. 3C, HSP27 is diffusely localized throughout the cytoplasm in control cells. The p38 immunostaining was dotted throughout control cells (Fig. 3E). After treatment of H460 cells with 20 μM aloe-emodin and 1.6 J/cm^2 light dose, a significant decrease in the fluorescent intensity of p38 protein was observed in the cytosol (Fig. 3F). Based on the above data, cells rapidly underwent cell death, which was induced by the disruption of the adhesion-derived signals after treatment of H460 cells with 20 μM aloe-emodin and 1.6 J/cm^2 light dose. Therefore, we verified that photosensitized aloe-emodin-induced H460 cell death is anoikis.

3.4. Photodynamic effects of aloe-emodin on apoptotic characteristics in H460 cells

To further investigate whether the induction of anoikis, a form of apoptosis, by aloe-emodin with irradiation was a typical apoptosis of H460 cells, the analysis of phosphatidylserine externalization was performed. It is well-known that apoptotic cells lose the asymmetry of the membrane phospholipid, which leaves phosphatidylserine on the outer leaflet of the plasma membrane. One of the tools for studying apoptosis is to quantify the phosphatidylserine externalization by binding of annexin V. Propidium iodide (PI) is a non-specific DNA intercalating agent, which is excluded by the plasma membrane of living cells, and thus can be used to distinguish necrotic cells from apoptotic. The annexin V/propidium iodide staining and flow cytometry analysis were used to confirm the photodynamic effect of aloe-emodin on apoptotic characteristics in H460 cells. The annexin V-FITC(−)/PI(−) population was regarded as control cells (Q3), whereas annexin V-FITC(+)/PI(−) cells were taken as a measure of early apoptosis (Q4), annexin V-FITC(+)/PI(+) as late apoptosis (Q2) and annexin V-FITC(−)/PI(+) as necrosis (Q1). As shown in Fig. 4A, cells treated for 4 h with aloe-emodin and irradiated with light resulted in a light dose-dependent increase in necrosis cells (Q1 area). Significant increase in necrosis cells was indicated by decreased proportion of cells in late apoptotic cells (Q2 area). Increasing the fluence dose to 0.4 J/cm^2 resulted in ~30% apoptotic and ~69% necrotic cells, whereas a higher light fluence, 1.6 J/cm^2, appeared to reduce apoptotic death while necrosis increased to nearly 81%. To further examine whether photoactivated aloe-emodin-induced H460 cell death is an apoptosis–necrosis switch, we determined plasma membrane permeability by PI staining. In this study, H460 cells were placed for 0, 30, 60 and 90 min in the dark after 4 h of incubation with 20 μM aloe-emodin followed by light irradiation and then the cells were immediately stained by 5 μM PI for 5 min. As shown in Fig. 4B, we demonstrated that photoactivation of aloe-emodin caused a cell death mode switch from apoptosis to necrosis, depending on the duration of the aloe-emodin-photosensitized cells placed in the dark.

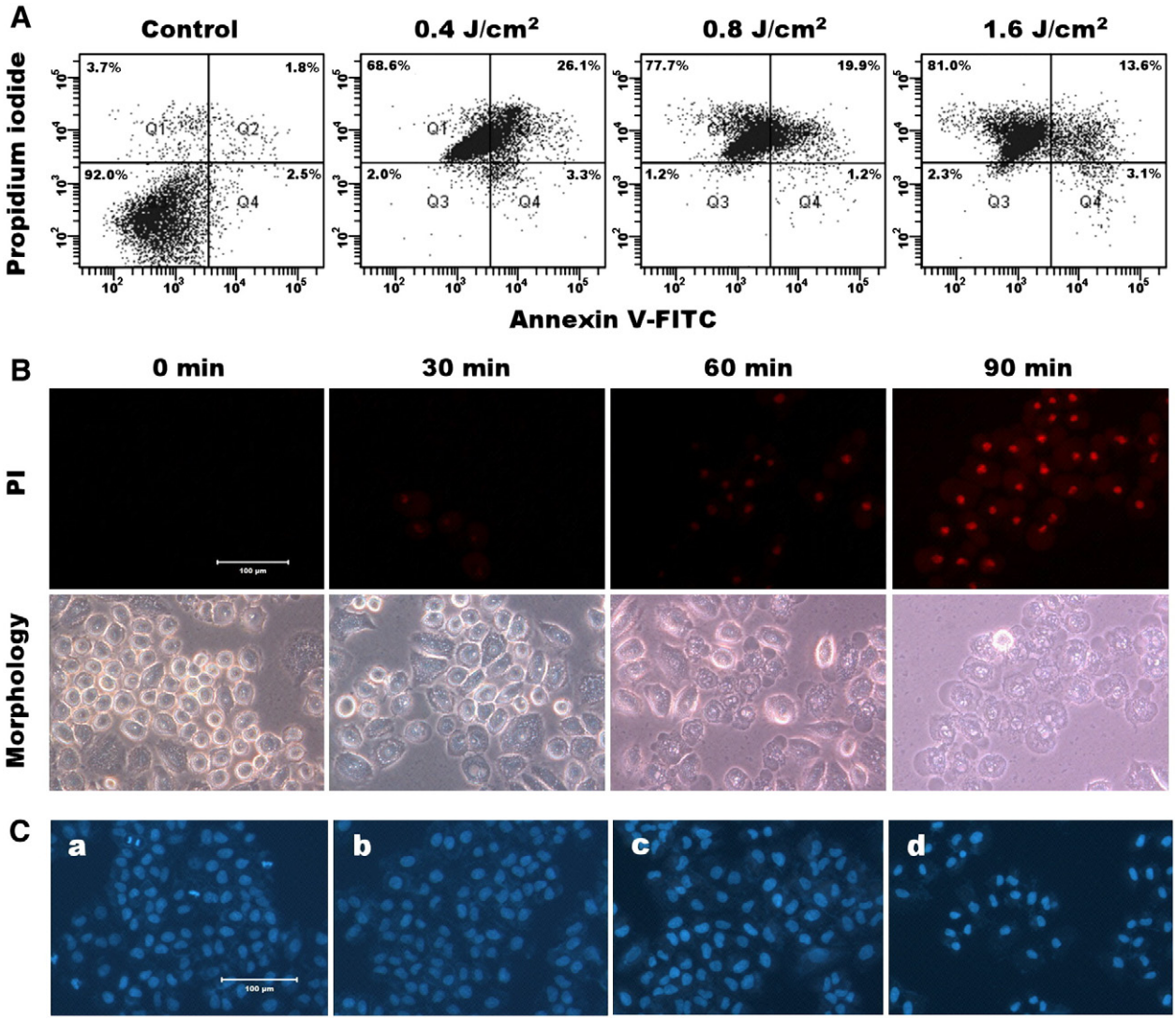

Fig. 4. Photoactivation of aloe-emodin induced H460 cell apoptosis. (A) The effect of aloe-emodin with irradiation on phosphatidylserine externalization of H460 cells. Cells were incubated with 0.1% DMSO or 20 μM aloe-emodin followed by irradiation with 0.4, 0.8 and 1.6 J/cm^2 fluence dose. Cells were then processed for annexin V-FITC/PI staining and analyzed with flow cytometry. (B) Photodynamic effects of aloe-emodin on plasma membrane integrity of H460 cells. H460 cells were incubated with 20 μM aloe-emodin for 4 h and then irradiated with 1.6 J/cm^2 fluence dose. After irradiation, cells were placed for 0, 30, 60 and 90 min in the dark and then the cells were immediately stained with 5 μM propidium iodide (PI) for 5 min at 37 °C. The cells were observed by fluorescence microscopy. (C) Aloe-emodin with irradiation induced phenotypic changes in cell nucleus. H460 cells were incubated with 0.1% DMSO (c) or 20 μM aloe-emodin (d) for 4 h and then irradiated with 1.6 J/cm^2 fluence dose. After irradiation, cells were stained with DAPI and then examined by fluorescence microscopy. In light-shield condition, cells were incubated with 0.1% DMSO (a) or 20 μM aloe-emodin (b) for 4 h. All results are representative of three independent experiments.

To further confirm whether photoactivated aloe-emodin-induced cell death is apoptosis of H460 cells, the analysis of nuclear morphology, evidenced by the DAPI staining, was performed. As shown in Fig. 4C, pretreatment with 20 μM aloe-emodin for 4 h and then irradiated with 1.6 J/cm^2 light dose resulted in a significant change in nuclear morphology of H460 cells. The nucleus is smaller than that of control cells. Based on the above data, photosensitized aloe-emodin-induced H460 cell death is apoptosis while cells rapidly undergo apoptosis–necrosis switch.

3.5. Photoactivated aloe-emodin-induced anoikis is mediated through the intrinsic and extrinsic death pathways in a caspase-dependent manner in H460 cells

To obtain further support for the induction of apoptosis by photoactivation of aloe-emodin, we examined the mitochondrial function, which is an indicator of the intrinsic pathway of apoptosis. To confirm the possible involvement of mitochondrial function in the process of photoactivated aloe-emodin-induced apoptosis, we measured the opening of mitochondrial permeability transition (MPT) pore in intact cells by flow cytometry. The opening of MPT pores was detected by the calcein loading-Co^{2+} quenching technique. As shown in Fig. 5, treatment with 20 μM aloe-emodin for 4 h and irradiation with 1.6 J/cm^2 light dose resulted in a decrease in calcein fluorescence intensity due to the opening of MPT pores. In this study, cells treated with aloe-emodin and irradiated with 1.6 J/cm^2 light dose showed a significant increase in the expression of apoptosis-inducing factor and cytochrome *c* (Fig. 6). We also determined the protein expression of caspase family members that mediated cell death pathway. Photoactivated aloe-emodin triggered a significant decrease in the protein expression of proform caspase-3 and -7 in H460 cells (Fig. 6). However, the protein levels of proform of caspase-8 and -9 were markedly increased after treatment with aloe-emodin and irradiation (Fig. 6). The expression of apoptosis-related proteins, such as Bcl-2 and Bax, was also examined in this study. Photoactivation of aloe-emodin resulted in significant decreases in Bcl-2 protein levels in H460 cells (Fig. 6). It is interesting to notice that Bcl-2 phosphorylation and fragmentation were induced after photodynamic treatment

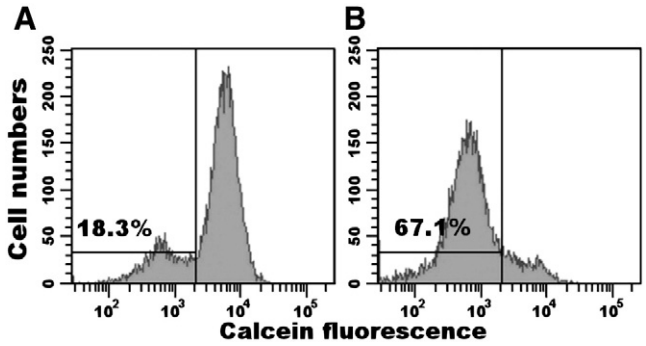

Fig. 5. Photoactivation of aloe-emodin caused the opening of mitochondrial permeability transition (MPT) pore in H460 cells. Cells were loaded with 1 μM calcein-AM for 30 min at 37 °C in DMEM medium containing 1 mM $CoCl_2$. After washing with PBS, H460 cells were incubated with 0.1% DMSO (A) or 20 μM aloe-emodin (B) for 4 h and then irradiated with 1.6 J/cm^2 fluence dose. After irradiation, the cells were harvested and then analyzed by flow cytometry for loss of fluorescence intensity due to efflux of the dye. Results are representative of three independent experiments.

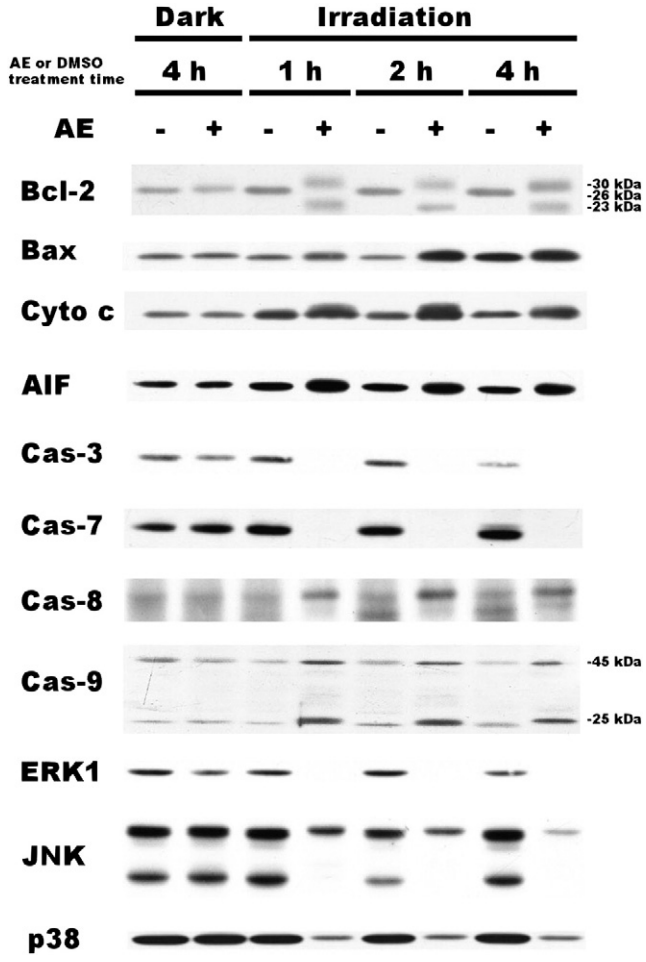

Fig. 6. Photodynamic effects of aloe-emodin on the expression of apoptosis-related proteins and MAP kinase members in H460 cells. The effects of photosensitized aloe-emodin on the protein levels of apoptosis-inducing factor (AIF), cytochrome *c* (Cyto c), Bcl-2, Bax, JNK, ERK1, p38 and caspase (Cas) family members were detected by Western blot analysis. H460 cells were incubated with 0.1% DMSO or 20 μM aloe-emodin for 1, 2 or 4 h and then irradiated with 1.6 J/cm^2 fluence dose. In light-shield condition, cells were treated with 0.1% DMSO or 20 μM aloe-emodin for 4 h. Cell lysates were analyzed by 10% (AIF and caspase-8), 12% (ERK1, JNK and p38), 13% (Bcl-2, caspase-3, -7 and -9) and 14% (Bax and cytochrome *c*) SDS-PAGE, and then probed with primary antibodies as described in Section 2. −: control cells; +: aloe-emodin-treated cells. Results are representative of three independent experiments.

(Fig. 6). The amount of Bax protein significantly increased after treatment with 20 μM aloe-emodin and irradiation with 1.6 J/cm^2 light dose (Fig. 6). Collectively, these data suggest that photoactivation of aloe-emodin induces anoikis through the intrinsic and extrinsic death pathways in H460 cells.

3.6. Photodynamic effects of aloe-emodin on protein expression of MAP kinase family members in H460 cells

In order to elucidate the role of MAP kinase family members in photoactivated aloe-emodin-induced H460 cell anoikis, the protein expression of MAP kinase family members in H460 cells was examined by Western blot analysis. When cells were incubated with 20 μM aloe-emodin prior to irradiation, the levels of ERK1, JNK and p38 significantly decreased at all time (Fig. 6). In the dark, aloe-emodin (20 μM, 4 h) had no effect on the protein expression of JNK, ERK1 and p38 (Fig. 6). These results suggested that JNK pathway plays a role in the anoikis induced by aloe-emodin with irradiation in H460 cells.

4. Discussion

Understanding the mechanisms of different photosensitizers and the influence of photosensitizer on cancer cells may provide more information in designing new photodynamic therapy strategies for cancer therapy. Since aloe-emodin was found to be a photosensitizer and possess anti-tumor activity, we investigated the mechanisms of photoactivated cytotoxicity of aloe-emodin in H460 cells. The present study demonstrated that treatment with 20 μM aloe-emodin for 4 h and 1.6 J/cm^2 light dose resulted in a marked photocytotoxicity of H460 cells. Aloe-emodin did not show any dark toxicity at the 20 μM concentration and 4 h incubation in H460 cells. In addition, we also verified that the effect of aloe-emodin on photocytotoxicity is more potent than that of 5-aminolevulinic acid, which is a second generation photosensitizer, in H460 cells.

Anoikis is a specific type of cells rapidly undergoing apoptosis induced by loss of adhesion (Frisch and Screaton, 2001). Resistance to anoikis may be an important early characteristic of malignant cancer and therefore represents a therapeutic target for the prevention of cancer metastasis and neoplastic growth. Furthermore, mechanisms that trigger anoikis in tumor cells are of potential interest in designing anti-tumor therapies (Bharadwaj et al., 2005; Rocco and Sidransky, 2001). Since H460 cells displayed a rounded morphology and rapidly formed large membrane blebs after treatment with aloe-emodin and fluence dose, we identified that photosensitized aloe-emodin-induced cell death might be anoikis in this study. After photodynamic treatment, apoptotic characteristics such as nuclear condensation, externalization of phosphatidylserine and apoptotic bodies were observed in H460 cells. Therefore, photoactivated aloe-emodin-induced anoikis is also a typical apoptosis. In this study, photoactivation of aloe-emodin induced significant changes in protein levels of proform caspase-3, -7, -8 and -9, which are important indicators of apoptosis. Our results are consistent with the notion that anoikis is mediated through the extrinsic (involving caspase-8) and the intrinsic (involving caspase-9) apoptotic pathways (Aoudjit and Vuori, 2001; Valentijn et al., 2003). We also demonstrated that photosensitized aloe-emodin induced a significant reduction of mitochondrial membrane potential in H460 cells. In addition, photoactivation of aloe-emodin significantly increased the protein expression of cytochrome *c* and apoptosis-inducing factor in this study. Although cells rapidly underwent anoikis induced by treatment with aloe-emodin and light, apoptosis was virtually the unique type of cell death in response to photosensitized aloe-emodin in H460 cells in this study.

This study demonstrated that Bax overexpression was involved in photoactivated aloe-emodin-induced anoikis in H460 cells. It is

worthy of note that exposure of H460 cells to aloe-emodin and fluence dose resulted in significant decreases in Bcl-2 protein levels which was accompanied by a significant increase in the phosphorylation and cleavage of Bcl-2. Consistent with such results, other studies have suggested that Bcl-2 phosphorylation is related to the triggering of apoptosis (Ling et al., 2002; Srivasted et al., 1999). Cheng et al. (1997) also demonstrated that cleavage of Bcl-2 occurred at NH_2-terminal loop domains by caspases, including caspase-8 and -9, and such proteolysis cleavage leads to Bax-like pro-apoptotic activity. The result of the production of Bcl-2 cleavage is consistent with that of caspase-8 and -9 protein expression, which significantly increased after treatment with aloe-emodin and fluence dose of H460 cells.

Anoikis is induced following the loss of cell–cell or cell–extracellular matrix interaction (Grossmann, 2002). Therefore, many intracellular events, including the assembly of focal adhesion, actin microfilament reorganization and recruitment of many signaling molecules to the focal adhesions were involved in the anoikis or apoptosis (Leung et al., 2008; Soldani et al., 2007). In this study, photoactivation of aloe-emodin reduced the amount of F-actin and induced stress fiber formation in H460 cells. Microtubules and actin microfilaments are the major proteins of cytoskeleton and both regulate cell shape. We also demonstrated that photoactivation of aloe-emodin significantly induced the disruption of microtubules. It is worthy of note that the photoactivated aloe-emodin-induced changes in the distribution of α-actinin, which is an actin-cross-linking protein, were comparable to that of control cells. These results indicated that the photoactivated aloe-emodin-induced anoikis and changes in cell morphology were mediated in part through its effect on cytoskeleton in H460 cells.

Activation of MAP kinase family members has been implicated in the regulation of apoptotic cell death. Okada et al. (2005) have also indicated that p38 MAP kinase-mediated F-actin reorganization promotes apoptotic cell death. According to the results of immunostaining experiments and Western blot analysis, the protein amount of p38 significantly decreased after aloe-emodin and irradiation. HSP27 has also been known as a downstream target protein of p38 (Nofer et al., 2006). It has been reported that p38-mediated F-actin reorganization was associated with translocation of HSP27 from cytosolic to cytoskeletal fraction (Okada et al., 2005). HSP27 is a component of the large and heterogeneous group of chaperone proteins, and its main functions are inhibition of apoptosis and prevention of protein aggregation (Sarto et al., 2004). Many investigators indicated that stress-induced HSP27 translocation into the nucleus is required for the more rapid disaggregation of nuclear proteins that were denatured and aggregated by stress (Borrelli et al., 1996; Kampinga et al., 1994). In this study, H460 cells showed a significant re-distribution of HSP27 from cytosol to nucleus during photosensitized aloe-emodin-induced anoikis. It indicated that the translocation of HSP27 from cytosol to nuclear resulted in a decrease in regulatory potency of HSP27 in F-actin reorganization. It also seemed to suggest that it is necessary for HSP27 to enter the nucleus and directly perform a function therein to achieve its maximal level of stress protection, but not cooperate with p38 to the reorganization of F-actin. In addition, exposure of H460 cells to aloe-emodin and fluence dose resulted in decreases in the protein levels of ERK1 and JNK. Based on the above data, MAP kinase members are important regulators of the photosensitized aloe-emodin-induced apoptosis in H460 cells.

In summary, this study has shown that photosensitized aloe-emodin can rapidly induce H460 cell death. Photoactivation of aloe-emodin induces either apoptosis or necrosis, depending on the light-activating dose. Since cytoskeletal potentially alteration is involved in the photosensitized aloe-emodin-induced rapid cell death, we verified that the photoactivated aloe-emodin-induced H460 cell death is anoikis, that is, apoptosis. Anoikis induced by aloe-emodin-irradiation is associated with the protein expression of MAP kinase members. Photoactivation of aloe-emodin induces a rapid opening of the mitochondrial permeability transition pore and change in cytochrome *c* protein expression. We also demonstrated that the photosensitized aloe-emodin-induced anoikis is mediated through the intrinsic and extrinsic death pathways in a caspase-dependent manner in H460 cells.

Acknowledgements

This work was supported by National Science Council Grant NSC 97-2320-B-039-005-MY3 and China Medical University Grant CMU97-174 of the Republic of China.

References

Aoudjit, F., Vuori, K., 2001. Matrix attachment regulates Fas-induced apoptosis in endothelial cells: a role for c-flip and implications for anoikis. J. Cell Biol. 152, 633–643.

Bais, H.P., Vepachedu, R., Lawrence, C.B., Stermitz, F.R., Vivanco, J.M., 2003. Molecular and biochemical characterization of an enzyme responsible for the formation of hypericin in St. John's wort (*Hypericum perforatum* L.). J. Biol. Chem. 278, 32413–32422.

Bharadwaj, S., Thanawala, R., Bon, G., Falcioni, R., Prasad, G.L., 2005. Resensitization of breast cancer cells to anoikis by tropomyosin-1: role of Rho kinase-dependent cytoskeleton and adhesion. Oncogene 24, 8291–8303.

Borrelli, M.J., Lepock, J.R., Frey, H.E., Lee, Y.J., Corry, P.M., 1996. Excess protein in nuclei isolated from heat-shocked cells results from a reduced extractability of nuclear proteins. J. Cell. Physiol. 167, 369–379.

Cárdenas, C., Quesada, A.R., Medina, M.A., 2006. Evaluation of the anti-angiogenic effect of aloe-emodin. Cell. Mol. Life Sci. 63, 3083.

Castano, A.P., Mroz, P., Hamblin, M.R., 2006. Photodynamic therapy and anti-tumour immunity. Nat. Rev. Cancer 6, 535–545.

Cheng, E.H.Y., Kirsch, D.G., Clem, R.J., Ravi, R., Kastan, M.B., Bedi, A., Ueno, K., Hardwick, J.M., 1997. Conversion of bcl-2 to a bax death effector by caspases. Science 278, 1966–1968.

Debnath, J., Mills, K.R., Collins, N.L., Reginato, M.J., Muthuswamy, S.K., Brugge, J.S., 2002. The role of apoptosis in creating and maintaining luminal space within normal and oncogene-expressing mammary acini. Cell 111, 29–40.

Frisch, S.M., Francis, H., 1994. Disruption of epithelial cell–matrix interactions induces apoptosis. J. Cell Biol. 124, 619.

Frisch, S.M., Screaton, R.A., 2001. Anoikis mechanisms. Curr. Opin. Cell Biol. 13, 555–562.

Grossmann, J., 2002. Molecular mechanisms of "detachment-induced apoptosis—anoikis". Apoptosis 7, 247.

Jones, B.U., Helmy, M., Brenner, M., Serna, D.L., Williams, J., Chen, J.C., Milliken, J.C., 2001. Photodynamic therapy for patients with advanced non-small-cell carcinoma of the lung. Clin. Lung Cancer 3, 37–41.

Kajitani, N., Kobuchi, H., Fujita, H., Yano, H., Fujiwara, T., Yasuda, T., Utsumi, K., 2007. Mechanism of A23187-induced apoptosis in HL-60 cells: dependency on mitochondrial permeability transition but not on NADPH oxidase. Biosci. Biotechnol. Biochem. 71, 2701–2711.

Kampinga, H.H., Brunsting, J.F., Stege, G.J., Konings, A.W., Landry, J., 1994. Cells overexpressing Hsp27 show accelerated recovery from heat-induced nuclear protein aggregation. Biochem. Biophys. Res. Commun. 204, 1170–1177.

Lee, H.Z., Hsu, S.L., Liu, M.C., Wu, C.H., 2001. Effects and mechanisms of aloe-emodin on cell death in human lung squamous cell carcinoma. Eur. J. Pharmacol. 431, 287–295.

Lee, H.Z., Wu, C.H., Chang, S.P., 2005. Release of nucleophosmin from the nucleus: involvement in aloe-emodin-induced human lung non small carcinoma cell apoptosis. Int. J. Cancer 113, 971–976.

Leung, W.C., Hour, M.J., Chang, W.T., Wu, Y.C., Lai, M.Y., Wang, M.Y., Lee, H.Z., 2008. P38-associated pathway involvement in apoptosis induced by photodynamic therapy with *Lonicera japonica* in human lung squamous carcinoma CH27 cells. Food Chem. Toxicol. 46, 3389–3400.

Ling, Y.H., Liebes, L., Ng, B., Buckley, M., Elliott, P.J., Adams, J., Jiang, J.D., Muggia, F.M., Perez-Soler, R., 2002. PS-341, a novel proteasome inhibitor, induces Bcl-2 phosphorylation and cleavage in association with G2-M phase arrest and apoptosis. Mol. Cancer Ther. 1, 841–849.

McCaughan Jr., J.S., 1999. Survival after photodynamic therapy to non-pulmonary metastatic endobronchial tumors. Lasers Surg. Med. 24, 194–201.

Morton, C.A., Brown, S.B., Collins, S., Ibbotson, S., Jenkinson, H., Kurwa, H., Langmack, K., McKenna, K., Moseley, H., Pearse, A.D., Stringer, M., Taylor, D.K., Wong, G., Rhodes, L.E., 2002. Guidelines for topical photodynamic therapy: report of a workshop of the British Photodermatology Group. Br. J. Dermatol. 146, 552–567.

Nofer, J.R., Noll, C., Feuerborn, R., Assmann, G., Tepel, M., 2006. Low density lipoproteins inhibit the Na+/H+ antiport in human platelets via activation of p38MAP kinase. Biochem. Biophys. Res. Commun. 340, 751–757.

Okada, T., Otani, H., Wu, Y., Kyoi, S., Enoki, C., Fujiwara, H., Sumida, T., Hattori, R., Imamura, H., 2005. Role of F-actin organization in p38 MAP kinase-mediated apoptosis and necrosis in neonatal rat cardiomyocytes subjected to simulated ischemia and reoxygenation. Am. J. Physiol. Heart Circ. Physiol. 289, H2310–H2318.

Rocco, J.W., Sidransky, D., 2001. p16(MTS-1/CDKN2/INK4a) in cancer progression. Exp. Cell Res. 264, 42–55.

Sarto, C., Valsecchi, C., Magni, F., Tremolada, L., Arizzi, C., Cordani, N., Casellato, S., Doro, G., Favini, P., Perego, R.A., Raimondo, F., Ferrero, S., Mocarelli, P., Galli-Kienle, M., 2004. Expression of heat shock protein 27 in human renal cell carcinoma. Proteomics 4, 2252–2260.

Schwartz, M.A., 1997. Integrins, oncogenes, and anchorage independence. J. Cell Biol. 139, 575–578.

Soldani, C., Croce, A.C., Bottone, M.G., Fraschini, A., Biggiogera, M., Bottiroli, G., Pellicciari, C., 2007. Apoptosis in tumour cells photosensitized with Rose Bengal acetate is induced by multiple organelle photodamage. Histochem. Cell Biol. 128, 485–495.

Srivasted, R.K., Mi, Q.S., Hardwick, J.M., Longo, D., 1999. Deletion of the loop region of Bcl-2 completely blocks paclitaxel-induced apoptosis. Proc. Natl. Acad. Sci. U. S. A. 96, 3775–3780.

Swan, E.A., Jasser, S.A., Holsinger, F.C., Doan, D., Bucana, C., Myers, J.N., 2003. Acquisition of anoikis resistance is a critical step in the progression of oral tongue cancer. Oral Oncol. 39, 648–655.

Valentijn, A.J., Metcalfe, A.D., Kott, J., Streuli, C.H., Gilmore, A.P., 2003. Spatial and temporal changes in Bax subcellular localization during anoikis. J. Cell Biol. 162, 599–612.

Wu, R.W., Chu, E.S., Yow, C.M., Chen, J.Y., 2006. Photodynamic effects on nasopharyngeal carcinoma (NPC) cells with 5-aminolevulinic acid or its hexyl ester. Cancer Lett. 242, 112–119.

Zobayed, S.M., Afreen, F., Goto, E., Kozai, T., 2006. Plant–environment interactions: accumulation of hypericin in dark glands of *Hypericum perforatum*. Ann. Bot. (Lond) 98, 793–804.